Available online at www.sciencedirect.com
SCIENCE DIRECT®
ELSEVIER
Microporous and Mesoporous Materials 57 (2003) 121–131
MICROPOROUS AND MESOPOROUS MATERIALS
www.elsevier.com/locate/micromeso

Cu^{2+}-acetate and Cu^{2+}-ammine exchanged heulandite: a structural comparison

Thomas Armbruster [a,*], Petra Simoncic [a], Nicola Döbelin [a], Anna Malsy [a], Ping Yang [b]

[a] *Laboratorium für chemische und mineralogische Kristallographie, Universität Bern, Freiestrasse 3, CH-3012 Bern, Switzerland*
[b] *Department of Chemistry, Soochow University, Suzhou 215006, PR China*

Received 8 July 2002; received in revised form 12 August 2002; accepted 30 August 2002

Abstract

Natural heulandite crystals were transformed into the Na-form of composition $|Na_{8.6}(H_2O)_n|[Al_{8.6}Si_{27.4}O_{72}]$–HEU (NaHEU). The precursor phase was subsequently treated (1) with 0.36 M Cu^{2+}-acetate solution (pH = 6) for three months at 343 K (CuacHEU) and (2) with 1 M NH_3 solution (pH = 11) containing 0.025 M Cu^{2+} (cuprammine solution) for 24 days at 393 K (CuammHEU). Chemical analyses with an energy dispersive system of a SEM indicated for both Cu^{2+} exchanged batches complete removal of Na. However, for CuacHEU (light blue hue) 3.3 Cu per formula unit (pfu) and for CuammHEU (dark blue) only 2.2 Cu pfu were detected. Charge balance in CuacHEU was assumed to occur by additional extra-framework oxonium (H_3O^+) and by NH_4^+ in CuammHEU, respectively. The presence of NH_4^+ in CuammHEU was also shown by IR spectroscopy. Duplicate crystal structure refinements were performed for both samples in space group C2/m converging at R1 = 0.048 (CuacHEU) and R1 = 0.038 (CuammHEU). The major Cu sites in both structures have no bonds to framework oxygen. In CuacHEU 45% of Cu is found in the center of the ten-membered A channel forming a disordered $[Cu(H_2O)_6]^{2+}$ complex. In the eight-membered B channel 43% of the total Cu forms an approximately square planar H_2O complex. In CuammHEU 49% of Cu is in the center of the A channel forming a disordered square planar Cu^{2+}-tetraammine complex $[Cu(NH_3)_4]^{2+}$ with two additional H_2O molecules (Cu–O: 2.5 Å) completing the Cu coordination to a strongly elongated octahedron. The Cu arrangement in the B channel of CuammHEU is very similar to CuacHEU.

Keywords: Natural zeolites; Heulandite; Clinoptilolite; Cu-exchange; Single-crystal X-ray structure refinement; Cu^{2+} acetate; Cuprammine complex

1. Introduction

Heulandite-type zeolites (HEU) comprise heulandite and clinoptilolite with the simplified formulas $|(Na,K)Ca_4(H_2O)_{24}|\,[Al_9Si_{27}O_{72}]$–HEU and $|(Na,K)_6(H_2O)_{20}|\,[Al_6Si_{30}O_{72}]$–HEU [1]. Distinction between heulandite and clinoptilolite is done on the basis of the Si/Al ratio, silica-rich crystals (Si/Al > 4.0) are clinoptilolites and the more aluminous ones (Si/Al ⩽ 4.0) are heulandites [2,3]. Both minerals represent naturally occurring zeolites with a high degree of Si, Al disorder. The

* Corresponding author. Fax: +41-31-631-3996.
E-mail address: thomas.armbruster@krist.unibe.ch (T. Armbruster).

1387-1811/02/$ - see front matter
PII: S1387-1811(02)00559-0

crystal structure (space group C2/m, $a \approx 17.7$, $b \approx 17.9$, $c \approx 7.4$ Å, $\beta \approx 116°$) exhibits three types of structural channels confined by tetrahedral ring systems leading to two-dimensional pathways parallel to (0 1 0) for zeolite-like diffusion. Strongly oblate ten-membered *A*-rings and more circular eight-membered *B*-rings confine the A and B channels running parallel to the *c*-axis (Fig. 1). Eight-membered *C*-rings border C channels running parallel to [1 0 0] and [1 0 2].

Clinoptilolite occurs as authigenic silicate mineral in large deposits, mainly of volcanoclastic origin, to be excavated at low cost by simple mining techniques [4]. The applications [5,6] range from wastewater treatment, aquacultural and agricultural applications, to catalytic cracking (mainly in the former Soviet Union). However, natural clinoptilolite rocks are (1) rather inhomogeneous and often composed of additional admixed phases (e.g., other zeolites, SiO_2, feldspars, clays, Fe-oxides/hydroxides) and (2) clinoptilolite is mostly fine crystalline in the 1 μm range. For a better understanding of HEU applications, the pure material is required and for single-crystal X-ray experiments large crystals are demanded. On such terms heulandite is more favorable because of its occurrence as individual large crystals in fissures of volcanic and metamorphic rocks.

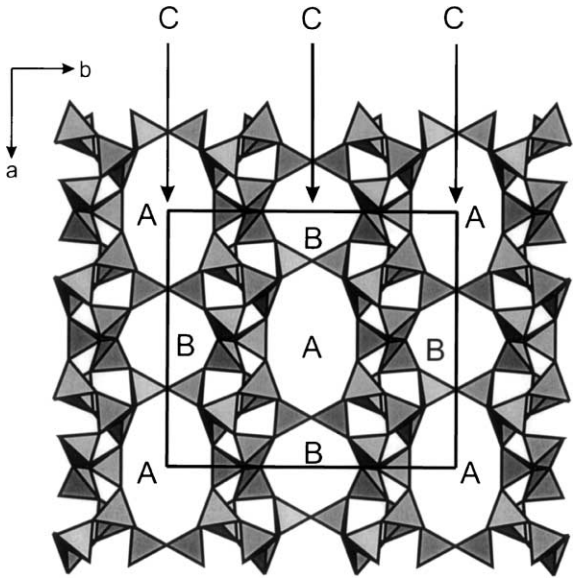

Fig. 1. Tetrahedral model of the heulandite framework projected along the *c*-axis, showing the ten-membered A and the eight-membered B channels. Eight-membered C channels, indicated by arrows, connect A and B channels.

The influence of monovalent cations (Na, K, Rb, Cs, NH_4, Ag) exchanged into the structure of heulandite was systematically investigated [7–9]. Furthermore, exchange of divalent cations (Mg, Mn, Cd, Sr, and Cu) using acidic salt solutions led to partial dealumination of heulandite, and only low concentrations of extra-framework cations could be incorporated and analyzed [10]. To avoid partial framework dealumination the exchange must be carried out in neutral or alkaline solutions as shown for Cd^{2+} and Pb^{2+} exchange [11,12]. Cu incorporation in HEU type zeolites has gained interest (1) from an environmental point of view for cleaning wastewaters from heavy metals (e.g., [13–18]) and (2) for a better understanding of how small divalent transition metals bond into the structural voids of zeolites [19,20]. In addition, Cu-exchanged zeolites display high activities for the decomposition of NO.

First experiments using a cuprammine solution for cation exchange of clinoptilolite were performed by Barrer and Townsend [21] applying NH_4-exchanged clinoptilolite as precursor phase. Upon cuprammine treatment (54 days at room temperature) fine crystalline clinoptilolite adopted the composition $|Cu^{2+}_{2.5}(NH_3)_{7.8}(NH^+_4)_{0.7}Ca_{0.7}(H_2O)_{16}|$ $[Al_{6.0}Fe_{0.3}Si_{29.7}O_{72}]$–HEU. Cu^{2+}-acetate exchange on heulandite-Na precursor crystals was attempted by Godelitsas et al. [19] at room temperature (seven days), but complete Cu-exchange was not achieved and the crystals still contained about 50% of the original Na. Based on EXAFS experiments it was concluded that Cu^{2+} is in sixfold coordination with Cu–O distances of 1.88(2) Å. This qualitatively confirms heulandite Cu^{2+}-exchange experiments for which single-crystal X-ray experiments located a $Cu(H_2O)^{2+}_6$ complex in the center of the A channel [10] as also found for Mg and Mn^{2+} in heulandite. Cu^{2+}-doped synthetic clinoptilolite with a variety of extra-framework cocations was studied by electron spin resonance and electron spin echo modulation spectroscopy [20]. It was found that the coordination of trace Cu^{2+} strongly depends on the type of co-cation.

The aim of the present study is (1) to produce a Cu^{2+} rich heulandite via cation exchange and (2) to study location and coordination of extra-framework Cu^{2+} by single-crystal X-ray methods. Structural studies of this type have the advantage over spectroscopic studies (e.g., ESR and EXAFS) that multiple Cu sites can directly be distinguished.

2. Experimental

2.1. Sample treatment

Natural, Ca-rich heulandite single crystals from Nasik, India [22] were crushed and sieved to 150–400 μm grains, which were placed in a 4 M NaCl solution in a Teflon autoclave at 423 K for four months, renewing the solution nine times to obtain Na-exchanged heulandite. Complete Na-exchange was verified by energy-dispersive analyses using a scanning electron microscope (SEM). The precursor phase had the composition $|Na_{8.6}(H_2O)_n|[Al_{8.6}Si_{27.4}O_{72}]$–HEU.

Sample CuacHEU was obtained by subsequent treatment in a 0.36 M Cu^{2+}-acetate solution (pH = 6) for 10 days at 393 K. However, under these conditions a light blue precipitate formed, which was dissolved by treating the sample with $CuSO_4$ solution of pH = 3. Subsequently the solution was replaced by 0.36 M Cu^{2+}-acetate solution (pH = 6) and the exchange was continued at 343 K for three months, renewing the solution once a month. Afterwards, the crystals were stored at room temperature in dilute Cu^{2+}-acetate solution for another three months. Complete Cu-exchange was verified by the absence of the Na specific line in the energy-dispersive spectrum of a SEM. The same type of analysis indicated ≈3.3 Cu per formula unit (pfu). The exchanged crystals had a faint turquoise—light blue hue. In addition, a turquoise colored precipitate (probably Cu^{2+}-acetate) decorated cracks within the crystals.

For preparation of a $[Cu(NH_3)_x]^{2+}$ form of heulandite (samples CuammHEU1 and CuammHEU2) the Na-exchanged crystals were treated with cuprammine solution [21]. The exchange solution was prepared by dissolving 1.2 g of $Cu^{2+}(NO_3)_2 3H_2O$ (Merck) in 200 ml of 1 M NH_3 solution (Hänseler) leading to a 0.025 M Cu^{2+} solution. The pH of this deep blue cuprammine solution was about 11. About 0.5 g of the Na-exchanged heulandites were placed in 50 ml of the cuprammine solution in a glass vessel that was closed to prevent evaporation. The crystals were exchanged during 50 days at room temperature, renewing the solution every 10 days. The samples were washed with diluted NH_3 solution and dried for 24 h. Quantitative energy dispersive analyses of individual crystals with the SEM showed only little incorporated copper (2.51 wt.% CuO) and still up to 2.10 wt.% Na_2O. For X-ray experiments, complete exchange of sodium was required and therefore the ion-exchange was continued at higher temperature.

The crystals (CuammHEU1), which were already partly exchanged at room temperature, were placed with 50 ml of the cuprammine solution in teflon-coated autoclaves at 393 K for 24 days, renewing the solution twice. Crystals without previous treatment at room temperature (CuammHEU2) were also exchanged with cuprammine solution at the same conditions as crystals of sample CuammHEU1. After 24 days the crystals, which changed from colorless to dark "ink" blue, were also analyzed with the SEM. Crystals from both samples had up to 6.9 wt.% CuO. Sodium was completely removed in both samples. In both samples heulandite was accompanied by a dark blue precipitate which was analyzed to be $Cu(OH)_2$. Because of the almost identical appearance and chemical composition samples CuammHEU1 and CuammHEU2 were not further distinguished and labeled CuammHEU.

2.2. Sample analyses

Two crystals from each synthesis (CuacHEU and CuammHEU) were selected for single-crystal X-ray structural investigation. The double experiments were performed to test whether crystals from the same batch also revealed identical (within statistical limits) arrangements of extra-framework cations and H_2O molecules. X-ray data collection was performed at room temperature with an Enraf Nonius CAD4 single-crystal X-ray diffractometer

using graphite monochromatized MoKα X-radiation. Because results of the double experiments led to almost identical results only details for one crystal each are presented (Table 1). Data reduction including Lorenz and polarization corrections were performed with the program package SDP [23]. All data were corrected for anisotropic absorption by empirical ψ-scans. Structure refinement was performed with the program SHELXL97 [24] using neutral-atoms scattering factors (Si for all tetrahedral sites—labeled T sites). Test refinements were preformed in space groups C2/m, Cm, and C2. Final data are presented for space group C2/m and the acentric space groups (C2 and Cm) were disregarded because of strong correlations among atomic sites related by the inversion operation. Refinements were carried out with anisotropic displacement parameters for all framework sites and highly populated extra-framework positions. Distinction between partially occupied Cu sites and light extra-framework atoms (O, N) was guided by interatomic distances and characteristic low displacement parameters for Cu. Direct distinction between NH_3, NH_4^+, H_2O, and H_3O^+ is not possible because these cations or molecules have almost identical numbers of electrons. Furthermore, H_2O and NH_3 show similar interatomic distances to Cu^{2+} and H_3O^+, NH_4^+, and H_2O occupy similar extra-framework sites [8].

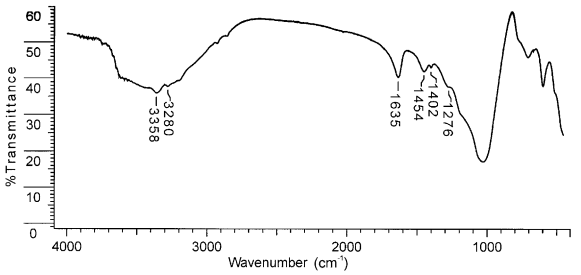

Fig. 2. IR powder spectrum (KBr pellet method) of sample CuammHEU. The absorptions at 1402 and 1454 cm^{-1} are characteristic of NH_4 whereas the shoulder at 1276 cm^{-1} has previously been assigned to an asymmetric deformation of NH_3 coordinated to Cu^{2+} [28,29].

Table 1
X-ray data collection and refinement parameters for Cu^{2+} treated heulandite

Sample	CuacHEU	CuammHEU
Crystal size (mm)	$0.27 \times 0.27 \times 0.07$	$0.40 \times 0.32 \times 0.10$
Diffractometer	Enraf Nonius CAD4	Enraf Nonius CAD4
X-ray radiation	fine focus sealed tube, MoKα	fine focus sealed tube, MoKα
X-ray power	50 kV, 40 mA	50 kV, 40 mA
Temperature	293 K	293 K
Space group	C2/m	C2/m
Cell dimensions *a*, *b*, *c* (Å)	17.639(6), 18.011(6), 7.426(3)	17.714(3), 18.074(2), 7.420(1)
β (°)	115.88(1)	115.99(1)
Absorption correction	Empirical ψ scans	Empirical ψ scans
Maximum 2θ	54.05°	49.96°
Measured reflections	3051	4689
Index range	$-22 \leqslant h \leqslant 21$; $-1 \leqslant k \leqslant 22$; $-1 \leqslant l \leqslant 8$	$-21 \leqslant h \leqslant 19$; $-21 \leqslant k \leqslant 21$; $-1 \leqslant l \leqslant 8$
Unique reflections	2333	1944
Reflections $> 2\sigma I$	1828	1795
R_{INT}	0.026	0.037
R_σ	0.042	0.032
Number of l.s. parameters	216	218
GooF	1.091	1.135
R_1, $F_o > 4\sigma(F_o)$	0.0477	0.0384
R_1, all data	0.0669	0.0425
wR_2 (on F_o^2)	0.1489	0.1004
Cu pfu located	3.5	2.5

$R_{INT} = \Sigma|F_o^2 - F_o^2(\text{mean})|/\Sigma F_o^2$, $R_\sigma = \Sigma\sigma(F_o^2)/\Sigma F_o^2$, $R_1 = \Sigma||F_o| - |F_c||/\Sigma|F_o|$, $wR_2 = \{(\Sigma w[F_o^2 - F_c^2]^2/\Sigma w[F_o^2]^2)\}^{1/2}$, Goof $= \{(\Sigma[wF_o^2 - F_c^2]/[n-p])\}^{1/2}$, $w = 1/(\sigma^2[F_o^2] + [0.04P]^2)$, $P = (\max(F_o^2, 0) + 2F_c^2)/3$.

An IR powder spectrum of sample CuammHeu was measured with a Perkin Elmer spectrometer using the KBr-pellet method (Fig. 2).

3. Results

3.1. Structure refinements

Atomic coordinates, populations, and equivalent isotropic displacement parameters are given in Tables 2 and 3. Both structures show within two standard deviations the same mean T–O bond lengths where Al is predominantly concentrated on T2 leading to mean T2–O of 1.649(3) Å. All other mean T–O distances vary between 1.618(3) for T4 and 1.631(3) for T3. The strong similarity of the T–O distances in both structures corroborates that CuacHEU crystals were not significantly dealuminated during the short-time acidic $CuSO_4$ treatment. Notice that partial dealumination in heulandite crystals is not reflected in the bulk Al concentration but leads to a rearrangement of framework Al to extra-framework Al [25].

In the structure of CuacHEU 3.5 Cu pfu were located of which 45% are concentrated in the center of the A channel on two sites, Cu1 (population 0.71) and Cu1′ (population 0.05) separated

Table 2
Atomic positional parameters, occupancies, and B_{eq} (Å^2) values for CuacHEU

Atom[a]	Occupancy	x/a	y/b	z/c	B_{eq} (Å^2)
T1		0.17888(6)	0.17058(5)	0.0973(1)	1.16(2)
T2		0.28320(6)	0.08897(5)	0.4918(1)	1.19(2)
T3		0.29474(6)	0.30891(5)	0.2875(1)	1.19(2)
T4		0.43357(6)	0.20016(6)	0.5829(1)	1.23(2)
T5		0	0.22107(8)	0	1.33(2)
O1		0.2998(3)	0	0.5367(7)	2.54(8)
O2		0.2704(2)	0.3794(2)	0.3896(5)	2.96(6)
O3		0.3164(3)	0.3445(2)	0.1133(5)	3.32(7)
O4		0.2294(2)	0.1029(2)	0.2473(4)	2.68(5)
O5		1/2	0.1717(3)	1/2	2.82(9)
O6		0.0807(2)	0.1665(2)	0.0567(5)	2.47(6)
O7		0.3802(2)	0.2697(2)	0.4547(5)	3.51(6)
O8		0.0110(2)	0.2747(2)	0.1851(4)	2.91(6)
O9		0.2164(2)	0.2510(2)	0.1919(5)	2.84(6)
O10		0.3761(2)	0.1295(2)	0.5771(5)	3.07(6)
CU1 A	0.71(1)	0	0	1/2	4.69(8)
CU1′ A	0.05(1)	0.000(1)	0	0.641(5)	3.2(6)[b]
CU2 A	0.052(5)	0	0.077(2)	0	5.4(8)[b]
CU3 A	0.056(4)	0.2031(9)	0	0.054(2)	2.7(4)[b]
CU4 B	0.392(4)	0.4055(1)	0	0.0549(4)	3.80(6)
OW2 A	1.00	0.1281(7)	0	0.667(2)	11.9(4)
OW4 A	0.355(4)	0.033(3)	0.063(3)	0.318(6)	26.53(7)
OW4′ A	0.355(4)	−0.0031(9)	0.1043(7)	0.403(3)	6.2(4)
OW8 A	0.42(3)	0.064(2)	0	0.135(5)	9.1(5)[b]
OW8′ A	0.35(2)	−0.074(2)	0	0.019(5)	9.1(5)[b]
OW1′ C	0.98(2)	0.2864(8)	0	0.031(2)	9.9(4)
OW3 B	0.88(2)	0.3999(5)	0.1017(5)	0.026(1)	9.9(2)
OW6 B	0.22(2)	0.475(2)	0	0.425(4)	4.2(7)[b]
OW9 B	0.35(5)	0.541(1)	0	0.220(4)	4.1(8)[b]
OW10 B	0.26(3)	0.508(2)	0	0.334(5)	9.1(5)[b]
OW11 B	0.24(5)	0.515(4)	0	0.071(9)	9.1(5)[b]
OW13 B	0.28(3)	0.537(2)	0.038(3)	0.158(6)	9.1(5)[b]

[a] Note, capital letters (A, B, C) after the atom symbol of extra-framework sites represent channel positions.

[b] Atoms with esd's in parentheses were refined isotropically. Anisotropically refined atoms are given in the form of the isotropic equivalent displacement parameter defined as $B_{eq} = 8/3\pi^2\Sigma_i(\Sigma_j(U_{ij}a_i * a_j * a_i.a_j))$.

Table 3
Atomic positional parameters, occupancies, and B_{eq} (Å^2) values for CuammHEU

Atom[a]	Occupancy	x/a	y/b	z/c	B_{eq} (Å^2)
T1		0.17847(5)	0.17018(5)	0.0962(1)	1.20(1)
T2		0.28494(5)	0.08898(5)	0.4921(1)	1.31(2)
T3		0.29173(5)	0.30911(5)	0.2850(1)	1.22(1)
T4		0.43247(5)	0.20160(5)	0.5817(1)	1.29(1)
T5		0	0.21923(7)	0	1.41(2)
O1		0.3009(3)	0	0.5360(6)	2.61(7)
O2		0.2670(2)	0.3792(2)	0.3848(4)	2.83(5)
O3		0.3143(2)	0.3441(2)	0.1121(4)	2.86(5)
O4		0.2290(2)	0.1035(2)	0.2474(4)	2.76(5)
O5		1/2	0.1764(2)	1/2	2.97(7)
O6		0.0799(2)	0.1649(2)	0.0496(4)	2.51(5)
O7		0.3754(2)	0.2696(2)	0.4511(4)	3.39(5)
O8		0.0147(2)	0.2723(2)	0.1874(4)	3.09(5)
O9		0.2141(2)	0.2513(2)	0.1892(4)	2.55(5)
O10		0.3782(2)	0.1291(2)	0.5738(5)	2.86(5)
CU1 A	0.599(6)	0	0	1/2	5.91(8)
CU3 B	0.152(5)	0.4019(4)	0	0.0660(9)	3.9(1)
CU4 B	0.079(3)	0.5341(5)	0.0331(6)	0.209(2)	5.1(2)
N11 A	0.24(4)	−0.130(1)	0	0.353(5)	3.2(8)[b]
N12 A	0.44(5)	−0.130(1)	0	0.257(6)	6.8(8)[b]
N2 A	0.35(4)	0.000(1)	0.1057(8)	0.444(3)	4.9(5)[b]
N/O22 A	0.24(4)	0.009(2)	0.097(2)	0.372(7)	5.8(9)[b]
OW2 A	0.38(3)	0.061(1)	0	0.108(4)	8.2(9)[b]
OW3 A	0.67(5)	0.069(2)	0	0.268(6)	18.1(14)[b]
OW5 A	0.45(4)	−0.057(2)	0	0.244(5)	15.9(17)[b]
OW1 C	0.49(4)	0.309(2)	0	0.089(7)	15.1(15)[b]
N/O31 C	0.66(4)	0.261(1)	0	0.955(2)	5.2(4)
OW6 B	0.79(2)	0.4043(7)	0.0947(6)	0.051(2)	15.9(3)
OW6a B	0.79(2)	1/2	0.055(2)	0	12.6(19)[b]
OW4 B	0.19(2)	0.451(3)	0	0.058(4)	4.27(8)[b]
N/O14 B	0.68(2)	0.491(2)	0	0.428(3)	10.7(5)
OW7 B	0.06(3)	0.523(4)	0	0.09(1)	2.6(29)[b]

[a] Note, capital letters (A, B, C) after the atom symbol of extraframework sites represent channel positions.
[b] Atoms with esd's in parentheses were refined isotropically. Anisotropically refined atoms are given in the form of the isotropic equivalent displacement parameter defined as $B_{eq} = 8/3\pi^2\Sigma_i(\Sigma_j(U_{ij}a_i * a_j * a_i.a_j))$.

by 1.0 Å along the c-axis. Cu1 is positioned on the inversion center (Fig. 3) and therefore Cu1′ appears as a satellite position above and below Cu1 indicating translational disorder along c. Cu1 bonds four times to OW4 (2.03 Å) and four times to OW4′ (2.00 Å). This is interpreted as two rotational-disordered square bases of an octahedron where each basis is formed by (OW4, OW4′, OW4, OW4′). The apices of the octahedron are formed by OW2 with a distance of 2.05 Å to Cu. The rotational disorder around the OW2–Cu–OW2 axis is further supported by the strongly anisotropic smearing of OW4 and OW4′ (Fig. 4). OW2 is fully occupied (in contrast to Cu1) indicating that OW2 is also available if Cu1 is vacant concealing the exact Cu1–OW2 bonding distance. Furthermore, the mean-square atomic displacement parameters of Cu1 are parallel to the c-axis (0.12 Å^2) four-times larger than perpendicular to c. This smearing associated with the Cu1′ satellite positions confirms translational disorder parallel to c. Cu2 (occupancy 0.05) also situated in the A channel, contributing only 6% to the total Cu content, has two bonds of 2.07 Å to the tetrahedral framework. Due to the low occupancy of Cu2 coordinating H_2O molecules cannot be resolved. Cu3 is another low-occupied (occupancy 0.06) cation site in the A channel (Fig. 3) with two dis-

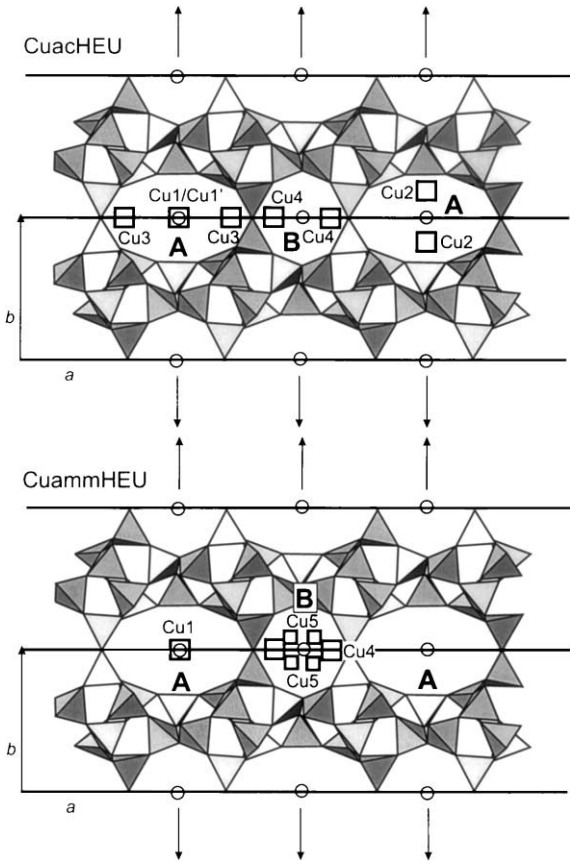

Fig. 3. Polyhedral model of a portion of the heulandite structure projected parallel to the *c*-axis with squares representing the Cu^{2+} extraframework sites. In addition, the prominent symmetry elements for space group C2/m are shown: small circles = center of inversion, heavy horizontal lines = traces of mirror planes, double-barbed arrows = twofold axes. Capital letters label the channel types.

tances of 2.27 Å to oxygen of the tetrahedral framework. The low population does not allow definition of a complete coordination.

Cu4 (occupancy 0.39) is in the B channel (Fig. 3) contributing 43% to the total Cu content. Cu4 has no bonds to the tetrahedral frameworks and possesses approximately square fourfold coordination with Cu–OW bonds between 1.84 and 2.03 Å. Exact Cu bonding distances are masked by H_2O disorder and higher occupancies of the H_2O ligands compared to the central Cu atom.

In the cuprammine exchanged crystal (CuammHEU) only 2.5 Cu^{2+} pfu were located (Fig. 3) agreeing with the measured chemical composition although 8.6 positive extra-framework charges were expected due to 8.6 Al pfu in the tetrahedral framework. Notice that all Na of the precursor phase was exchanged and we therefore assumed that additional NH_4^+ was incorporated to obtain charge balance. At pH = 11 the dominant hydrogenated nitrogen species is NH_3, but heulandite has a strong selectivity for NH_4^+. Evidence of NH_4^+ in cuprammine exchanged heulandite was also found by IR spectroscopy (see below). Comparison with completely NH_4^+-exchanged heulandite [8] led to the assignment of N31 (population 0.66(3)) and N14 (population 0.68(2)) as preferred NH_4^+ sites. If the corresponding populations are normalized per formula unit 5.4(2) positive charges are obtained. The excess above 3.6 positive charges (8.6^+–$2.5Cu^{2+}$) is interpreted as a mixed occupation of the potential NH_4^+ sites with H_2O or NH_3. The major Cu^{2+} concentration is located in the center of the A channel (Cu1, occupation: 0.60(1)) without any bonds to the tetrahedral framework (Fig. 3). The displacement ellipsoid of Cu1 reveals a cigar-like extension parallel to *c*. In addition, two groups of ligands 1.95–2.07 Å apart from Cu1 are located. N11 and N12 have almost identical *x* and *y* coordinates but are separated by 0.7 Å along *c*. The second group, formed by N2 and N/O22, shows a similar characteristic and is separated by 0.6 Å along *c*. Furthermore, N2 and N/O22 are duplicated by the twofold axis leading to four closely spaced positions, separated by 0.8 and 2 Å parallel to *c*. In a projection along the *c*-axis (Fig. 4) the N2 and either N11 or N12 ligands form a square around Cu1 interpreted as a copper tetraammine complex with translational disorder parallel to the *c*-axis (Fig. 4). The populations of disordered N11 and N12 sum up to 2.8(2) NH_3 pfu, about twice the value for Cu1 (1.2 pfu) as expected for the linear N11–Cu1–N11 or N12–Cu1–N12 bonding. The population of N2 alone yields 2.8(3) pfu as expected for the linear N2–Cu1–N2 unit (Fig. 4). Thus there is strong evidence that N/O22 does not belong to the copper tetraammine complex but is an additional NH_4^+ and/or H_2O site that is occupied if the center of the A channel is not occupied by Cu^{2+}. Additional evidence comes from the separation of N11 and

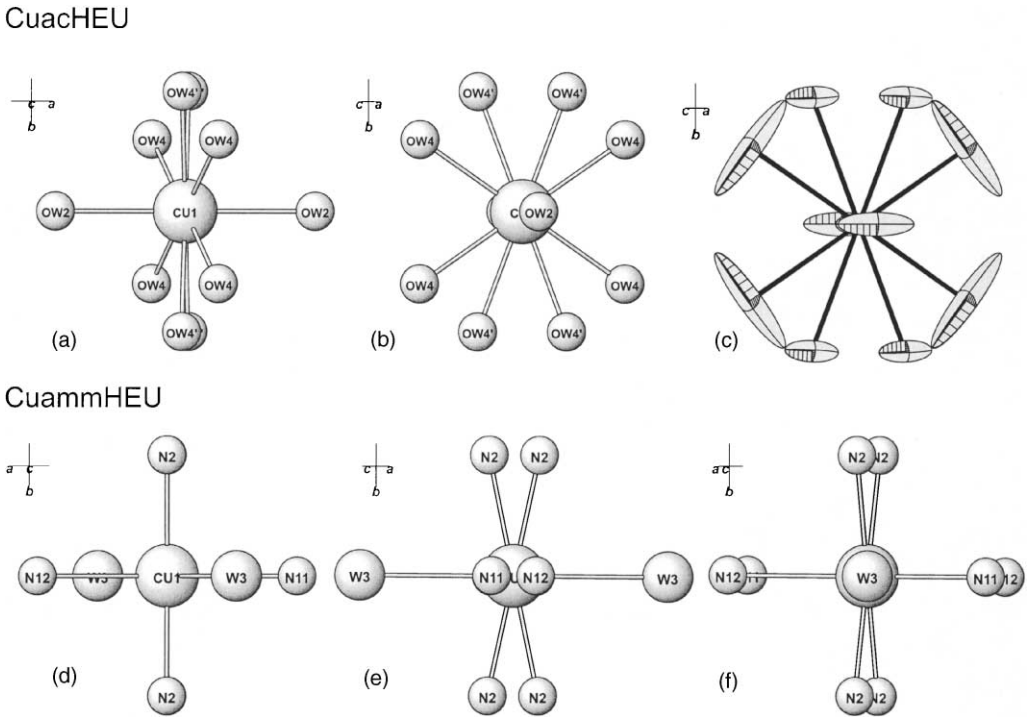

Fig. 4. (a) Coordination of Cu1 (sample CuacHEU) in the center of the A channel, projected parallel to the *c*-axis, showing a disordered $(Cu[H_2O]_6)^{2+}$ complex. All Cu1–OW distances are ≈2.0 Å long. The disorder can be described by rotating an approximate square base 45° around Ow2–Cu1–Ow2. (b) The same Cu1 coordination as in (a) but rotated 90° around *b*. The square base of the octahedron is formed by OW4–OW4′–OW4–OW4′ of which two orientations are visible. (c) The same orientation as (b) but displaying probability ellipsoids for all atoms. The pronounced smearing of the OW positions indicates librational disorder of the $(Cu[H_2O]_6)^{2+}$ complex mainly around the OW2–Cu1–OW2 axis. In addition, there is pronounced translational disorder parallel to *c* as evidenced by the elongation of the OW2 and Cu1 (hidden behind OW2) ellipsoids. (d) Coordination of Cu1 (sample CuammHEU) in the center of the A channel projected parallel to *c*. The cluster is interpreted as a disordered $(Cu[NH_3]_4)^{2+}$ complex with two distant (2.5 Å) H_2O molecules (W3) oriented approximately perpendicular to the cuprammine complex. The distance Cu–N is ≈1.95–2.07 Å. The disorder of the planar $(Cu[NH_3]_4)^{2+}$ complex, oriented in the *a*–*b* plane is mainly characterized by a translation parallel to *c*. For the attached NH_3 groups, translational disorder was modelled by multiple sites N11, N12 and N2, respectively. (f) projection of the disordered $(Cu[NH_3]_4)^{2+}$ complex along W3–Cu1–W3.

N12 (0.7 Å), which is similar to the splitting of N2 by the twofold axis causing a N2–N2 separation of 0.8 Å whereas N/O22–N/O22 are more than 2 Å apart. Assumption of translational displacement of the square complex parallel *c* requires similar displacements of the ligands. The copper tetraammine complex is further rounded out by two distant H_2O molecules (Cu1–OW3: 2.5 Å) completing the planar complex to a distorted octahedron (Fig. 4). The OW3 population, summing up to 2.7(2) pfu, is in excellent agreement with this interpretation. An independent indicator of the presence of a cuprammine complex in heulandite is the dark blue color of the CuammHEU crystals whereas CuacHEU crystals containing the $Cu[H_2O]_6^{2+}$ complex have a light-turquoise hue. In addition, there is a pronounced difference in the coordination of Cu1 between both structures. Cu4 in the B channel (contributing 25% to the total Cu content) has a similar environment as Cu4 in CuacHEU. Thus it remains questionable whether Cu4 is coordinated by NH_3 or by H_2O. Cu5, also in the B channel, is contributing 26% to the total Cu content and possesses a position slightly shifted from the mirror plane leading to a split position with a Cu5–Cu5 separation of 1.2 Å. Cu5 has one

distance of 2.41 Å to framework oxygen and exhibits only a poorly defined coordination to additional extraframework sites. Thus the true character of Cu5 cannot be unraveled.

3.2. IR spectrum of CuammHEU

An assignment of IR absorptions for HEU-type minerals, based on the general study by Flannigen et al. [26], has recently been published [27]. The strong absorption at 1053 cm^{-1} is due to asymmetric stretching of external linkages and the shoulder at 1205 cm^{-1} is due to asymmetric stretching of internal tetrahedra. In the spectrum of CuammHEU we observe an additional shoulder at 1276 cm^{-1} which was reported to be characteristic of the symmetric deformation of NH_3 coordinated to Cu^{2+} in Y-type zeolite [28] a corresponding band was also found for $[Cu(NH_3)_4]SO_4 \times H_2O$ [29]. The weak absorption at 1402 cm^{-1} was attributed to v_4 of NH_4^+ in NH_4-exchanged heulandite [8]. The stronger absorption at 1454 cm^{-1} is probably due to NH_4^+ on a different position [21]. The H_2O specific absorptions of K-exchanged heulandite appear at 3616, 3464 (broad, overlapping, poorly resolved) and at 1638 cm^{-1} [8]. Completely NH_4^+-exchanged heulandite has an additional strong v_3 (NH_4^+) absorption at 3134 cm^{-1}. The gap between the H_2O and NH_4^+ absorptions found for NH_4^+-exchanged heulandite is in cuprammine-exchanged heulandite covered by additional absorptions at ≈3358 and 3280 cm^{-1}. Thus the area between 2800 and 3700 cm^{-1} is characterized by a broad and poorly resolved overlay of several absorptions. The v_1 and v_3 (NH_3) absorptions for gaseous NH_3 are at 3336 and 3414 cm^{-1} [30] which is in fair agreement with the additional absorptions found in cuprammine exchanged heulandite. The v_4 (NH_3) absorption is expected at 1627 cm^{-1} [29] and is thus completely overlapping with v_2 (H_2O) at 1635 cm^{-1}.

4. Discussion

In an attempt to produce a completely Cu^{2+} exchanged heulandite from a Na-exchanged precursor phase, we succeeded in replacing all extra-framework Na. However, chemical analyses and single-crystal structure refinement showed that charge balance was not exclusively obtained by the substitution $Cu^{2+} \rightarrow 2Na^+$ because significantly less Cu^{2+} was found in the exchanged products. For exchange experiments using copper acetate solution of pH = 6 we speculate that charge balance was obtained by incorporation of $3.5Cu^{2+} + 1.6H_3O^+ \rightarrow 8.6Na^+$. If cuprammine solution (pH = 11) was applied the exchange reaction may be written $2.5Cu^{2+} + 3.6NH_4^+ \rightarrow 8.6Na^+$. The presence of NH_4^+ in addition to NH_3, complexing Cu^{2+}, was confirmed by IR spectroscopy. Cu^{2+} either coordinated by NH_3 or by H_2O strongly prefers extra-framework sites either in the A or in the B channel. Those positions are not bonded to framework oxygen sites. Godelitsas et al. [19], also using copper acetate solution for HEU exchange experiments, did not obtain complete replacement of Na. Using spectroscopic and bulk analytical methods they showed that Cu^{2+} is incorporated into heulandite via ion exchange. Furthermore, treatment of CuHEU with diethyldithiocarbamato ligands (Et_2dtc^-) and subsequent analyses by various spectroscopic methods disclosed the formation of a Cu^{2+}–Et_2dtc complex supported on the surface of the coarse crystalline heulandite substrate. These results raise the question whether the Cu^{2+}-doped synthetic clinoptilolites by Zhao et al. [20] were Cu^{2+} ion exchanged only on the surface or whether Cu^{2+} also penetrated into the structural voids. Zhao et al. [20] suggested on the basis of Cu^{2+} ESR and electron spin echo modulation spectroscopy that different sites are preferred by Cu^{2+} depending on the extra-framework co-cation. Furthermore, only partial hydration of Cu^{2+} was suggested. These results are not in agreement with the strongly Cu^{2+} exchanged samples investigated in this study. Based on our results two interpretations are suggested: (1) Short time Cu^{2+} doping of clinoptilolite leads to Cu^{2+} surface adsorption where Cu^{2+} bonds to framework oxygen and to H_2O. (2) In the presence of high concentrations of extra-framework co-cations (H, Na, K, Li) Cu^{2+} exhibits a different behavior and nestles either on less favorable cavity positions which were not already occupied by the dominant co-cations or the co-cations and their hydration

sphere provide suitable gaps to be occupied by Cu^{2+}. Zhao et al. [20] have chosen a Cu^{2+} doped sample since at higher copper-exchange levels spin-exchange interactions between paramagnetic ions makes it impossible to resolve the spectra of complexed and uncomplexed copper ions [27]. We may learn from a comparison of these results with our own data that the bonding behavior of trace concentrations are not transferable to highly exchanged samples.

Additional interesting insight is obtained by a comparison of the compositions of the cuprammine exchanged clinoptilolite by Barrer and Townsend [21] and our corresponding heulandite sample. Both samples exhibit very similar Cu^{2+} concentrations although the clinoptilolite [21] had 6 Al pfu in the framework, whereas our heulandite had 8.6 Al pfu. This may indicate that the increased Al content in heulandite is balanced by NH_4^+ which develops hydrogen bonds to framework oxygen adjacent to Al sites [8], whereas clinoptilolite with low Al, and also with less ordered Al, is more selective for NH_3-complexed Cu^{2+} without bonds to the tetrahedral framework. Thus the selectivity depends on both the Al concentration and its arrangement.

X-ray structure analysis of strongly exchanged samples has the advantage that this technique is "blind" for surface adsorptions and only resolves positions displaying a certain degree of translational order. Furthermore, multiple extra-framework positions can be located allowing for direct determination of their coordination, whereas in many spectroscopic techniques individual sites can either not be resolved or not unambiguously be attributed to a structural position. E.g., the average octahedral Cu–O distance of 1.88(2) Å extracted from EXAFS experiments [19] is rather short for mainly Cu^{2+}–H_2O interactions. Our diffraction results indicate ≈2.0 Å for octahedral Cu centered in the A channel. In addition, we have also located fourfold coordinated Cu^{2+} in the B channel, thus the EXAFS results must be considered an average over various sites of different coordinations.

However, there is also a strong disadvantage of the diffraction technique, in particular for the study of partially occupied extra-framework cation sites, characteristic of most zeolites with strongly disordered Si, Al distribution in the framework. A low occupied extra-framework cation site associated with a low occupied H_2O position does not necessarily mean that these sites bond to each other. It could also be that one site is only occupied if the other position is vacant and vice versa. In this case the interpretation is guided by an appropriate bonding distance and correlated occupancies of both sites.

This study also demonstrates the importance of investigations on zeolites with different degree of exchange (trace amounts versus dominant substitution) and emphasizes the necessity of analytical techniques which allow distinction between adsorption on the surface and incorporation into the structural channel or cavity system.

Both structure refinements in this study were performed in space group C2/m agreeing with the topological symmetry of the tetrahedral HEU framework and indicating strong Si, Al disorder. Previous exchange studies, using the same type of NaHEU precursor material, yielded after incorporation of Pb^{2+} [11], Cd^{2+} [12], and Cs^+ [7] lower diffraction symmetry, either Cm [11,12] or $C\bar{1}$ [7], also reflected in increased Si, Al order within the framework. Thus the symmetry resolution of the diffraction experiments mainly depends on the X-ray scattering power of the extra-framework occupants and on the main extra-framework positions of the strongly scattering occupants. In heulandite Cu^{2+} prefers a position in the A channel of local 2/m symmetry thus this symmetric arrangement does not allow to resolve lowering from average C2/m symmetry. However, there is no doubt that there is substantial short range Si, Al order as discussed by Kato et al. [31] based on modeling of ^{29}Si MSA NMR spectra. Furthermore, Akizuki et al. [32] found within one macroscopic "crystal" of heulandite domains of triclinic and monoclinic symmetry differing from growth sector to growth sector. In other words, each macroscopic heulandite crystal is composed of various polymorphs, distinct by different Si, Al ordering patterns, intergrown in a twin-like relationship [5]. This means that the diffraction experiment is only able to determine the space- (and time) averaged symmetry of a heulandite "crystal".

Acknowledgement

This study was supported by the Swiss National Science Foundation (grant 20-65084.01), which is highly appreciated.

References

[1] T. Armbruster, M.E. Gunter, in: D.L. Bish, D.W. Ming (Eds.), Reviews in Mineralogy and Geochemistry, vol. 45, Natural Zeolites: Occurrence, Properties, Applications, Mineralogical Society of America, 2001, pp. 1–56.
[2] D.S. Coombs, A. Alberti, T. Armbruster, G. Artioli, C. Colella, E. Galli, E.J.D. Grice, F. Liebau, J.A. Mandarino, H. Minato, E.H. Nickel, E. Passaglia, D.R. Peacor, S. Quartieri, R. Rinaldi, M. Ross, R.A. Sheppard, E. Tillmanns, G. Vezzalini, Can. Mineral. 35 (1997) 1571.
[3] D.L. Bish, J.M. Boak, in: D.L. Bish, D.W. Ming (Eds.), Reviews in Mineralogy and Geochemistry, vol. 45, Natural Zeolites: Occurrence, Properties, Applications, Mineralogical Society of America, 2001, pp. 207–216.
[4] R.L. Hay, R.A. Shepard, in: D.L. Bish, D.W. Ming (Eds.), Reviews in Mineralogy and Geochemistry, vol. 45, Natural Zeolites: Occurrence, Properties, Applications, Mineralogical Society of America, 2001, pp. 217–234.
[5] T. Armbruster, in: A. Galarnau, F. Di Renzo, F. Faujula, J. Vedrine (Eds.), Zeolites and Mesoporous Materials at the Dawn of the 21th Century, Studies in Surface Science and Catalysis, vol. 135, Elsevier, Amsterdam, 2001, pp. 13–27.
[6] R. Roque-Malherbe, in: H.S. Nalwa (Ed.), Handbook of Surfaces and Interfaces of Materials, vol. 5: Biomolecules, Biointerfaces, and Applications, Academic Press, 2001, pp. 496–522.
[7] P. Yang, T. Armbruster, J. Solid State Chem. 123 (1996) 140.
[8] P. Yang, T. Armbruster, Eur. J. Mineral. 10 (1998) 461.
[9] N. Bresciani-Pahor, M. Calligaris, G. Nardin, L. Randaccio, J. Chem. Soc. Dalton Trans. (1981) 2288.
[10] J. Stolz, T. Armbruster, in: C. Colella, F.A. Mumpton (Eds.), Natural Zeolites for the Third Millenium, De Frede-Editore, Naples, 2000, pp. 119–138.
[11] M.E. Gunter, T. Armbruster, T. Kohler, C.R. Knowles, Am. Mineral. 79 (1994) 675.
[12] J. Stolz, P. Yang, T. Armbruster, Micropor. Mesopor. Mater. 37 (2000) 233.
[13] M.J. Zamzow, B.R. Eichbaum, K.R. Sandgren, D.E. Shanks, Sep. Sci. Technol. 25 (1990) 1555.
[14] H. Kurama, M. Kaya, in: J.P. Hager, B. Mishra, C.F. Davidson, J.L. Litz (Eds.), Proceedings of Treatment and Minimization of Heavy Metal Containing Wastes, The Mineral and Metals and Materials Society, 1995, pp. 113–125.
[15] S.K. Ouki, M. Kavannagh, Waste Manage. Res. 15 (1997) 383.
[16] R. Pode, G. Burtica, V. Pode, A. Iovi, E. Popovici, in: I. Kiricsi, G. Pál-Brobély, J.B. Nagy, H.G. Karge (Eds.), Porous Materials in Environmentally Friendly Processes, Studies in Surface Science and Catalysis, vol. 125, Elsevier, Amsterdam, 1999, pp. 769–776.
[17] L. Curkovic, S. Cerjan-Stefanovic, T. Filipan, M. Modric, Kemija u Industriji 48 (1999) 441.
[18] L.Y. Li, Develop. Arid Reg. Res. 1 (2000) 675.
[19] A. Godelitsas, D. Charistos, J. Dwyer, C. Tsipis, A. Filippidis, A. Hatzidimitriou, E. Pavlidou, Micropor. Mesopor. Mater. 33 (1999) 77.
[20] D. Zhao, R. Szostak, L. Kevan, J. Phys. Chem. B 101 (1997) 5382.
[21] R.M. Barrer, R.P. Townsend, J. Chem. Soc. Faraday Trans. 1 (72) (1976) 2650.
[22] R.N. Sukheswala, R.K. Avasia, M. Gangopadhay, Mineral. Mag. 39 (1974) 658.
[23] Enraf-Nonius, Structure determination package (SDP), Enraf-Nonius, Delft, The Netherlands, 1983 (computer program).
[24] G.M. Sheldrick, SHELX-97, University of Göttingen, Germany, 1979 (computer program).
[25] T. Wüst, J. Stolz, T. Armbruster, Am. Mineral. 84 (1999) 1126.
[26] E.M. Flanigen, H. Khatami, H.A. Szymanski, Adv. Chem. Ser. 101 (1971) 201.
[27] G. Rodriguez-Fuentes, A.R. Ruiz-Salvador, M. Mir, O. Picazo, G. Quintana, M. Delgado, Micropor. Mesopor. Mater. 29 (1998) 269.
[28] D.R. Flentge, J.H. Lunsford, P.A. Jacobs, J.B. Uytterhoeven, J. Phys. Chem. 79 (1975) 354.
[29] B.N. Cyvin, S.J. Cyvin, K.H. Schmidt, W. Wiegeler, A. Müller, J. Mol. Struct. 30 (1976) 315.
[30] G. Herzberg, Molecular Spectra and Molecular Structure, II. Infrared and Raman Spectra of Polyatomic Molecules, D. Van Nostrand Comp, Princeton, New Jersey, 1945, p. 295.
[31] M. Kato, S. Satokawa, K. Itabashi, in: H. Chon, S.-K. Ihm, Y.S. Uh (Eds.), Progress in Zeolite and Microporous Materials, Studies in Surface Science and Catalysis, vol. 105, Part A, Elsevier, Amsterdam, 1997, pp. 229–235.
[32] M. Akizuki, Y. Kudoh, S. Nakamura, Can. Mineral. 37 (1999) 1307.